Laser and Particle Beams (2015), *33*, 331–338.
© Cambridge University Press, 2015 0263-0346/15
doi:10.1017/S0263034615000014

High-charge divergent electron beam generation from high-intensity laser interaction with a gas-cluster target

P. KOESTER,[1] G.C. BUSSOLINO,[1] G. CRISTOFORETTI,[1] A. FAENOV,[2,3] A. GIULIETTI,[1] D. GIULIETTI,[5,6] L. LABATE,[1,6] T. LEVATO,[1,7] T. PIKUZ,[2,4] AND L.A. GIZZI[1,6]

[1]Intense Laser Irradiation Laboratory, Istituto Nazionale di Ottica, Consiglio Nazionale delle Ricerche, Pisa, Italy
[2]Joint Institute for High Temperatures, Russian Academy of Science (RAS), Moscow, Russia
[3]Division for Photon Science and Technology, Institute for Academic Initiatives, Osaka University, Osaka, Japan
[4]Graduate School of Engineering, Osaka University, Osaka University, Osaka, Japan
[5]Dipartimento di Fisica, Università di Pisa, Pisa, Italy
[6]INFN Sezione di Pisa, Pisa, Italy
[7]Fyzikální ústav AV ČR v.v.i., Praha, Czech Republic

(Received 13 October 2014; Accepted 6 January 2015)

Abstract

We report on an experimental study on the interaction of a high-contrast 40 fs duration 2 TW laser pulse with an argon-cluster target. A high-charge, homogeneous, large divergence electron beam with moderate kinetic energy (~2 MeV) is observed in the forward direction. The results show that an electron beam with a charge as high as 12 nC can be obtained using a table-top laser system. It was demonstrated that the accelerated electron beam is suitable for a variety of applications such as micro-radiography of thin samples in a wide field of view. It can also be applied for *in vitro* dosimetry studies.

Keywords: Electron acceleration; Clusters; Femtosecond lasers; Electron radiography

1. INTRODUCTION

The generation of electron beams through laser-driven electron acceleration in an underdense plasma (Tajima & Dawson, 1979; Modena *et al*., 1995) is a promising approach for the next generation electron accelerators. The interaction of a high-intensity, ultra-short laser pulse with a gas-jet target was studied extensively in the past years (Malka *et al*., 2002; Giulietti & Labate, 2010). Recently a new type of target gas, the clusterized gas, has received much attention due to its unique properties (Tajima *et al.*, 1999; Abdallah *et al*., 2001; Kishimoto & Tajima, 2000; Kishimoto *et al.*, 2002; Magunov *et al*., 2003; Sakabe *et al*., 2004; Fukuda *et al*., 2004; 2007; 2009; Gavrilenko *et al*., 2006; Sherrill *et al*., 2006; Colgan *et al.*, 2008; 2011; Faenov *et al*., 2008; 2009; 2012; 2013; Kugland *et al.,* 2008*a*; 2008*b*; Hayashi *et al.*, 2011; Zhang *et al.*, 2011; 2012; Bussolino *et al*., 2013; Chen *et al*., 2013). Clusterized gas targets are characterized by a relatively low average density with localized regions of solid density (Boldarev *et al*., 2006; Jinno *et al*., 2013). Efficient laser pulse propagation and enhanced laser energy absorption were observed in clusterized gases for non-relativistic laser intensities (Kim *et al.*, 2006; Kugland *et al.,* 2008*a*; 2008*b*). Electron acceleration in clusterized targets to energies of several tens to hundreds of MeV was demonstrated experimentally for laser intensities above 10^{19} W/cm^2 (Fukuda *et al.*, 2007; Zhang *et al.*, 2012). Clusterized gas targets present some advantages with respect to the usual gas targets (Kim *et al.*, 2006; Chen *et al*., 2013). In fact, the increased laser absorption allows higher values of ionization degree and correspondently relatively higher electron density plasmas ($N_e \sim 10^{19}$–5×10^{20} cm^{-3}). The parameters of the plasmas thus produced are particularly favorable for the acceleration of high charge and energetic electron bunches. In fact, the maximum accelerating electric field, related to the plasma waves in which the acceleration process develops, scales as the square root of the plasma density and the charge of the accelerated electron bunches increases with the density. The typical charge of electron bunches produced in low-density gas-jet targets is of the order of a few tens to a few hundreds of pC (Mangles *et al.*, 2012), much

Address correspondence and reprint requests to: P. Koester, Consiglio Nazionale delle Ricerche – Istituto Nazionale Ottica, Via Moruzzi 1, 56124 Pisa, Italy. E-mail: petra.koester@ino.it

lower than the results obtained in clusterized gas reported in (Zhang *et al.*, 2012; Chen *et al.*, 2013) and here. These circumstances indicate that clustered gas jets can be considered very promising targets for innovative sources of high-charge bunches of energetic electrons.

Such sources could have several applications. Among them the development of compact electron injectors for conventional accelerators, characterized by a high-charge (nC) and with the supplementary advantage of an easy synchronization with other apparatus (e.g., a laser) for pump and probe experiments. Another immediate application is the direct utilization of bunches of the accelerated electrons for electron micro-radiography. Indeed, in the frame of the Charged Particle Radiography (Mangles *et al.*, 2006; Serbanescu & Fedosejevs, 2006; Merrill *et al.*, 2007; Faenov *et al.*, 2009; Schumaker *et al.*, 2013; Bussolino *et al.*, 2013), electron contact radiography is one of the possible approaches to the development of imaging techniques with high spatial resolution for thin objects, which is important for a variety of applications including imaging of biological samples. It requires an electron beam with relatively low energy (a few MeV), such that the penetration depth (range) of the electrons is of the order of the thickness of the sample. Homogeneity and high charge are additional important characteristics of the electron beam to be suitable for electron applications.

Here we report on the experimental results obtained from the interaction of a 2 TW laser pulse with an Ar cluster-gas target. A high-charge, divergent electron beam of modest energy (up to a few MeV) is observed in the forward direction and radiography of different objects with spatial resolution of about 50 μm is provided. We demonstrated that the high divergence of the accelerated electrons that characterize laser–plasma acceleration (LPA) in our experimental conditions is suitable for such application, allowing larger samples to be irradiated without the use of electron optics or diffusing/homogenizer devices.

2. EXPERIMENTAL SETUP

The experiment was performed at the Intense Laser Irradiation Laboratory of the CNR in Pisa. The laser system delivers pulses with an energy up to 100 mJ on target. In the described experiment, the energy on target was 80 mJ/pulse. The laser beam (800 nm, 40 fs) was focused by means of f/5 off-axis parabola into the gas-jet (See Fig. 1). The nominal peak laser intensity was 1.7×10^{18} W/cm^2 with a contrast of 5×10^8 on a nanosecond time scale. The supersonic gas-jet nozzle exit was 4 mm long and 1.2 mm wide and the laser was propagating parallel to the shorter edge of the nozzle. The laser was focused close to the edge of the gas-jet closest to the focusing optics, at a vertical distance of 0.5 mm from the nozzle exit plane. As discussed below, the gas used in the experiment was Ar at a backing pressure between 45 and 50 bars, sufficient to produce clusterization of the gas. A Kodak Lanex Regular scintillating screen (marked as (1) in Fig. 1) is mounted at a distance of about 15 cm from the gas-jet nozzle for the characterization of the spatial profile of the electron beam. An imaging system

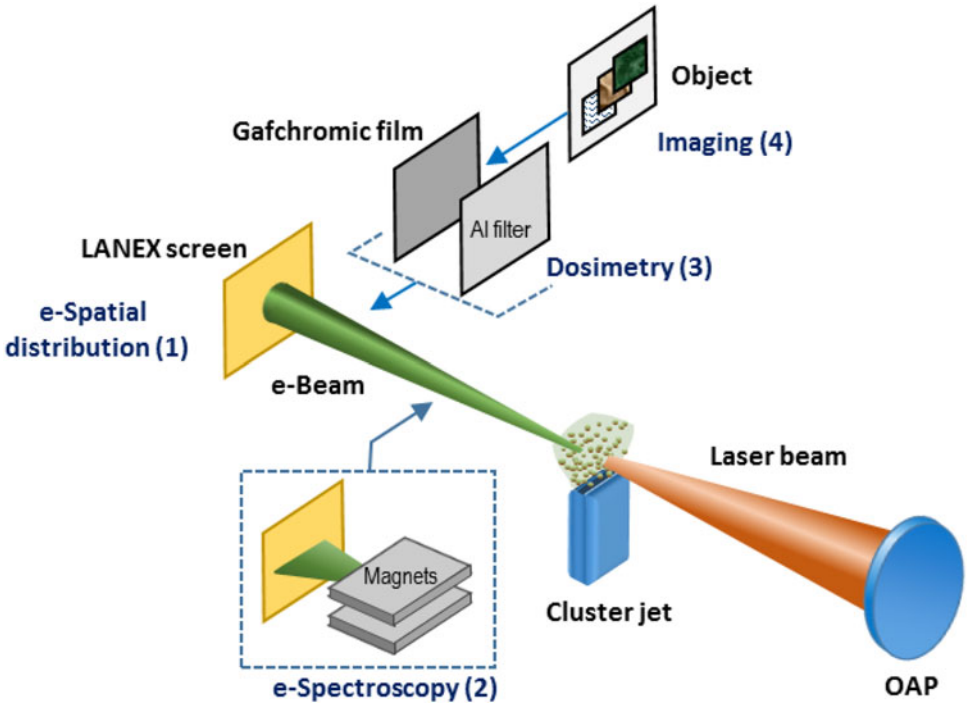

Fig. 1. Experimental setup. (1) Lanex screen used for the electron spatial distribution measurements; (2) magnetic spectrometer used for the measurements of the electron energy distribution; (3) Gafchromic film used for the electron beam charge measurements; (4) a complex object was placed in contact with the radiochromic film detector for e-radiography.

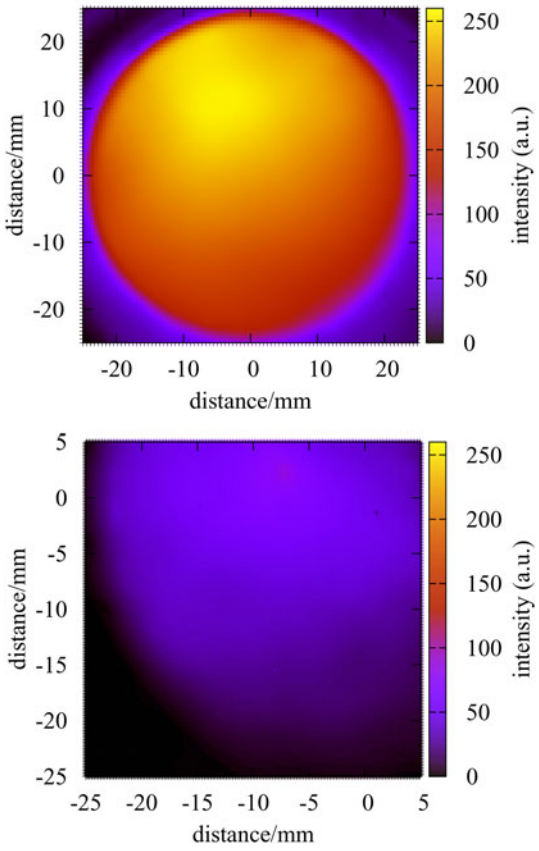

Fig. 2. Typical spatial distribution of the accelerated electron beam as detected by the scintillating screen at a distance of 15 cm from the gas-jet nozzle. The electron beam was obtained from the interaction of a 40 fs laser pulse at an intensity of 1.7×10^{18} W/cm^2 with an Ar-cluster target at a backing pressure of 46 bar (top) and an He gas target at a backing pressure of 40 bar (bottom).

is used to view the Lanex screen from outside the vacuum chamber. A magnetic spectrometer [marked as (2) in Fig. 1] with an entrance slit of 0.5 mm width is inserted between the nozzle and the Lanex screen at a distance of 8 mm from the Lanex screen for the characterization of the energy distribution of the accelerated electron beam. The charge of the electron beam is measured by means of a dosimetry film (Gafchromic MD-55) [marked as (3) in Figure 1]. A 15 μm thick Al filter is placed in front of the dosimetry film to avoid direct irradiation by the transmitted laser light and plasma self-emission.

3. EXPERIMENTAL RESULTS AND DISCUSSION

The spatial distribution of the electron beam detected by means of the scintillating screen as obtained from the interaction of a single laser pulse with an Ar-cluster target at a backing pressure of 46 bar is displayed in Figure 2 (top panel). The electron beam shows a very homogeneous spatial distribution over a wide region, well beyond the region imaged by the scintillating screen. In fact, in this case, the screen is set off-center, to image also the outer, lower intensity regions of the electron beam. Over the whole diameter of the scintillating screen of 5 cm the signal changes by less than a factor of two.

For comparison, in Figure 2 (bottom panel) the typical spatial distribution of the electron beam accelerated in an He gas target in the case of using 40 bar backing pressure is shown. In this case, the electron beam is less divergent (note the different spatial scales of the two panels) and less homogeneous. From the comparison of the Lanex signals in the two cases, it is evident that the total charge of the electron beam accelerated in He gas is much lower than in the case of the Ar-cluster target, as will be shown in the following.

For a detailed characterization of the spatial distribution of the electron beam in the case of the Ar-cluster target, a lineout along the diameter of the graph in Figure 2 (top panel) is shown in Figure 3 together with a Gaussian fit $f(x)=A\exp[(x-x_c)^2/(2\sigma^2)]$. The lineout of the data shows a smooth spatial profile and the width of the Gaussian fit

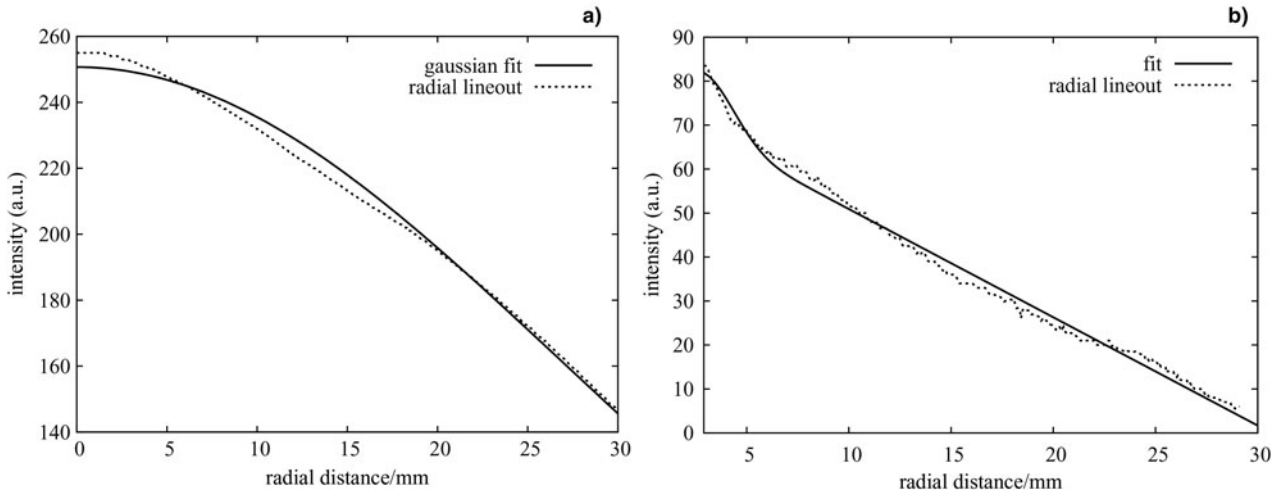

Fig. 3. Radial lineouts of the spatial distributions in Figure 2. The data obtained from the interaction with an Ar-cluster target was fitted with a Gaussian function (a) and the data obtained from the interaction with an He gas target with the sum of a Gaussian and a linear function (b).

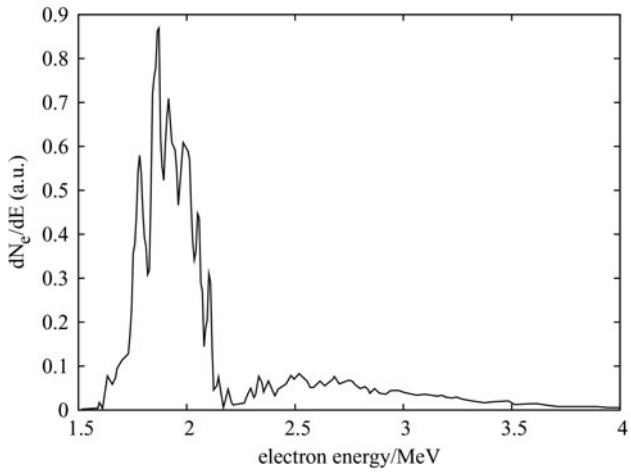

Fig. 4. Typical energy distribution of the electron beam obtained from the interaction of a 40 fs laser pulse at an intensity of 2×10^{18} W/cm^2 with an Ar-cluster target (backing pressure 46 bar). The sharp cut toward lower energies is due to the spectral limit of our spectrometer.

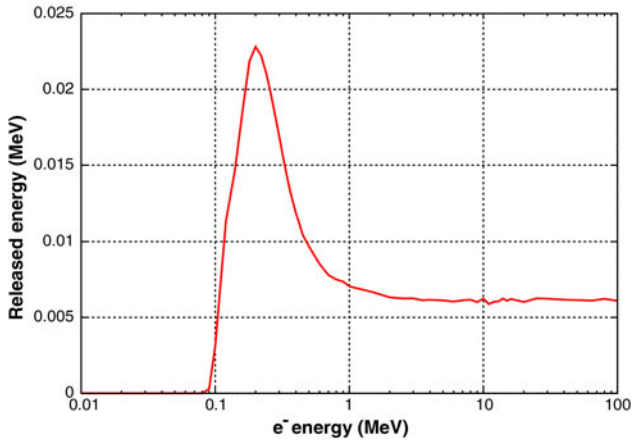

Fig. 5. Energy released in the active layers of a GAFCHROMIC MD-55 film as a function of incoming electron kinetic energy. The results are obtained from Monte Carlo simulations using Geant4 libraries for the experimental setup including an Al filter of 15 μm thickness.

results $\sigma = 26.8$ mm. Taking into account the distance from the nozzle to the scintillating screen the electron beam divergence is calculated to be 0.40 rad at full width at half maximum.

The energy distribution of the electron beam above the lower spectral limit of our spectrometer (1.5 MeV) is shown in Figure 4 for the electron beam generated in the Ar-cluster target. In this case, the backing pressure was 46 bar. The spectrum shows a bright peak at about 1.9 MeV with a low-intensity tail at higher energies. As for the shot to shot variability at the laser intensity above, the electron energy was found to be always above the detection limit and below the 2 MeV, with the details of the spectrum changing moderately from shot to shot.

Information on the total charge of the electron beam accelerated in the Ar-cluster target was retrieved through the analysis of the signal detected on a dosimetry film for a series of 36 pulses of the driving laser. Taking into account the response curve of Gafchromic MD-55 film (Chair *et al.*, 1998) and the measured optical density of the exposed film (OD = 0.77) we get a peak dose of about 25 Gy in the center of the spatial distribution of the electron beam. Considering the thickness (16 μm) of the two active layers and their density (1.08 g/cm^3) we can obtain the surface mass density and finally the energy released by the energetic electrons on the dosimetry film which is found to be 8.64×10^{-5} J/cm^2. A Monte Carlo simulation on the energy released by energetic electrons on MD-55 dosimetry film is reported in Figure 5.

As we can see, each 200 keV electron releases 22 keV, while an electron with energy of the order or greater than 1 MeV releases 6 keV. Thus the charge of the electron beam accelerated in the Ar-cluster target is in the range 5–18 nC, where the lower limit applies to a monoenergetic electron beam of 200 keV kinetic energy and the upper limit occurs for an electron beam with kinetic energy above 1 MeV. The electron energy distribution below 1 MeV was not measured during the experiment, as lower energy electrons are trapped inside the magnetic field of the spectrometer and thus are not detected on the Lanex screen. This generates a 50% uncertainty in the charge measurement of 12 ± 6 nC. From a comparison of the signal on the Lanex screen (Fig. 2) obtained in the case of the Ar-cluster target with the one obtained from He gas, the charge of the electron beam accelerated in He gas can be estimated. Both signals were integrated assuming circular symmetry. The charge of the electron beam obtained from the interaction of the laser pulse with the He target results to be of the order of 300 pC, more than one order of magnitude less than in the case of the Ar-cluster target. This value is consistent with values in literature, where the charge of the energetic electron beam, generated through laser-acceleration in gas targets, is typically of the order of tens to hundreds of pC (Mangles *et al.*, 2006). Electron beams with such high charge of several nC in the case of the Ar-cluster target were generated with a high degree of reproducibility. In a sequence of 101 laser shots, only 23 shots with significantly weaker fluorescence signal from the Lanex screen were registered resulting in a reproducibility of 77%. The generated electron beam was then used to irradiate a sample of a few centimeters size at contact with the radiochromic film detector. A detailed description of the radiographic results can be found in Bussolino *et al.* (2013). The spatial resolution was measured from the radiographic image of a sharp edge. Assuming a Gaussian point-spread-function, the RMS spot size was found to be 60 μm. It is necessary to stress the high sensitivity of the electron radiographic imaging in our case for low absorbing materials. As can be seen from Figure 6 (top left), Ni foils with a step thickness of only 10 μm could be clearly resolved despite of the fact that the total stopping range of 1 MeV electrons in Ni is about 680 μm. In Figure 6 (bottom right), a

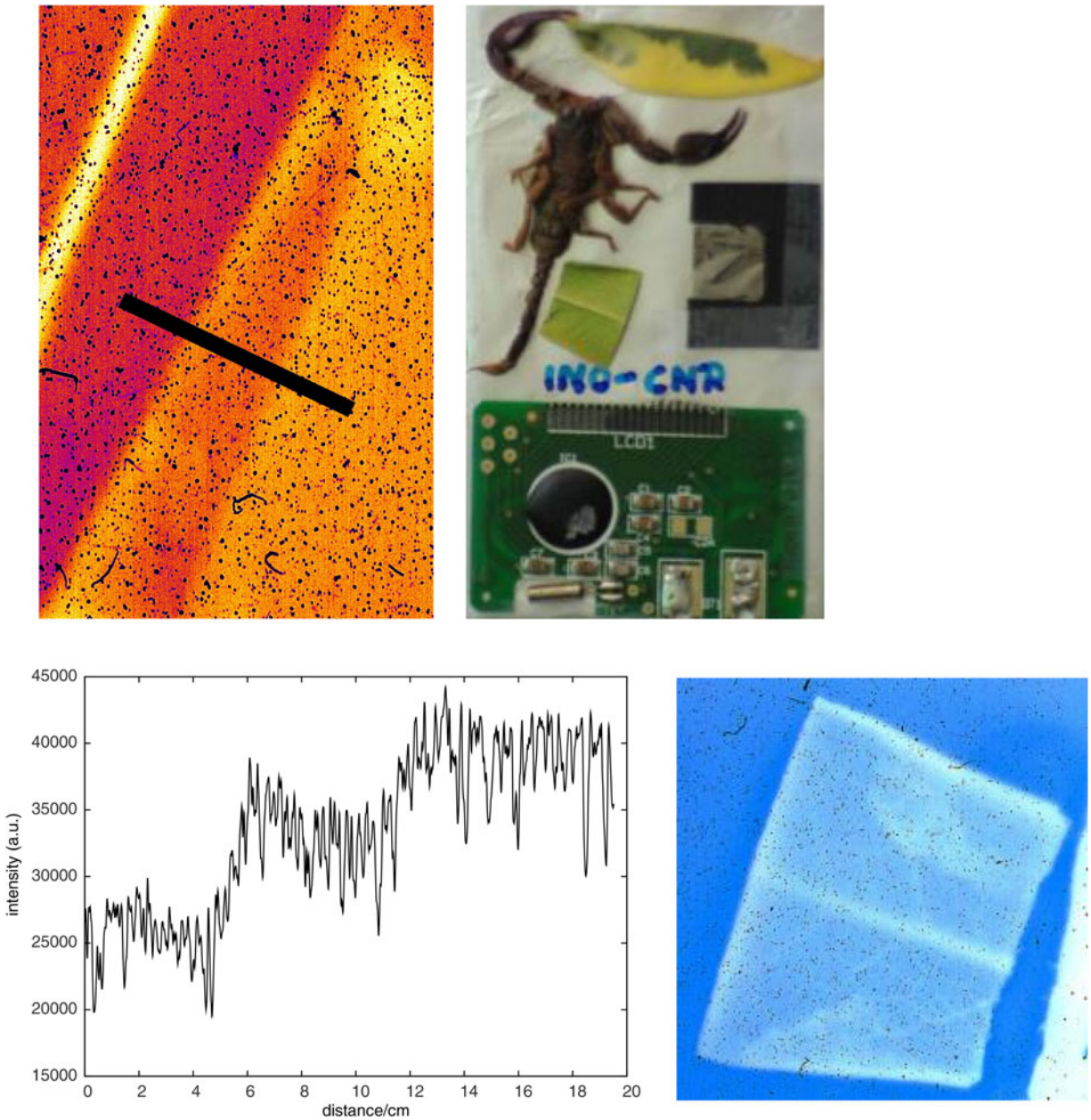

Fig. 6. Contact radiography performed with the electron beam obtained from the interaction of the laser pulse with the Ar-cluster target. Top left: Detail showing the radiography of two layers of a 10 μm thick Ni foil. The difference in absorption of 20 μm of Ni (light area), 10 μm of Ni (center diagonal), and no Ni (dark area) is visible. Bottom left: Lineout of the radiography in the top left panel along the black line. Top right: Photograph of one of the samples used for radiography. Bottom right: Detail (the leaf at the center) of the radiography of the sample in the top right panel. The internal structure of the leaf is visible.

detail of the radiography showing a leaf is displayed. Internal structures of the leaf, which had thickness about 100–200 μm, are clearly visible. A very important property of our electron radiography scheme is the wide field of view. In fact, the whole sample (see the photograph in Fig. 6, top right) having a size of several centimeters could be irradiated without displacing the sample.

These results on the characterization of the electron beam show that a high charge, homogeneous and divergent electron beam with moderate kinetic energy of 2 MeV can be generated through the interaction of the laser pulse with a clusterized Ar gas-jet target. It is therefore crucial to understand the role of clusters in this configuration.

In order to get information on the cluster parameters, simulations were performed for a conically shaped nozzle close to the one used in the experiments. The simulations show that Ar clusters with a radius between 40 nm (at 40 bar backing pressure) and 20 nm (at 60 bar) are generated. The concentration of clusters increases rapidly for backing pressures between 40 and 60 bar (see Fig. 7).

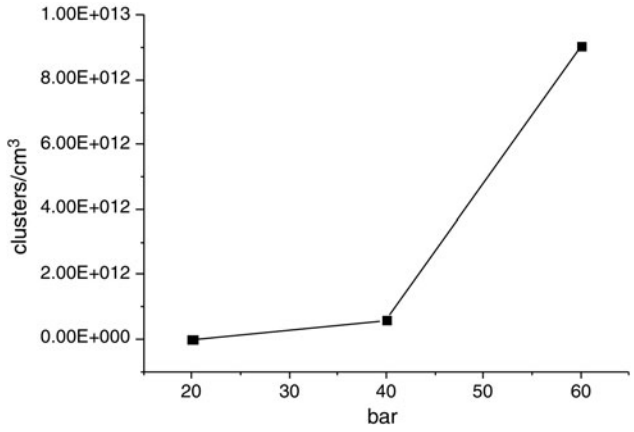

Fig. 7. Cluster density as a function of Ar gas backing pressure.

The efficient absorption of laser light in clusterized gases (Kishimoto & Tajima, 2001) leads to high ionization stages of the Ar atoms and thus to a high electron density (Magunov *et al.*, 2001; Sherrill *et al.*, 2006). Ionization stages up to 16 were reached in Ar-cluster targets for laser intensities similar to the ones used in the experiments (Abdallah *et al.*, 2001; Fukuda *et al.*, 2004; Faenov *et al.*, 2012). Thus, for a neutral gas density of 4×10^{19} cm^{-3} as expected for the used backing pressure, plasma electron densities above 10^{20} cm^{-3} are likely to be reached. This will contribute to increase the electron beam charge observed in the experiment. Given the very high electron density, strong self-focusing of the laser beam is expected to occur. In fact, the laser power of 2 TW largely exceeds the threshold power for self-focusing given by the relativistic critical power $P_c = \left(m_e c^5 \omega^2 / e^2 \omega_p^2\right) \approx 17 \left(\omega/\omega_p\right)^2$ GW, where m_e is the electron mass, c the speed of light, ω is the laser radiation angular frequency, e the electron charge and ω_p is plasma frequency ($P_c \approx 117$ GW for a density of 10^{20} cm^{-3}). Also, in our experimental conditions the laser pulse duration of 40 fs is much longer than the inverse of the plasma frequency $\omega_p^{-1} \sim 5$ fs. In these circumstances, the accelerating wake field is expected to be driven through self-modulation of the laser pulse (Najmudin *et al.*, 2003) in the case of a pure gas.

However, in the case of a cluster target, direct laser acceleration of the electrons contributes significantly to the overall energy gain as described in Chen *et al.* (2013) and confirmed there by two-dimensional fully electromagnetic particle in cell simulations. Modeling clearly showed that in the case of the clustering gas target the electron density distribution has a large bow-like structure and the electron density exhibits a strong modulation in a broad region directly following the laser pulse. It was also demonstrated that a big size plasma cavity appears in the central area, which heats the most energetic electrons and accelerate them. It was also shown by modeling in Chen *et al.* (2013) that in the case of a pure gas, the electron charge injected into wake fields and accelerated to the same energy is much lower. Simulations provided in Chen *et al.* (2013) demonstrated that the direct laser acceleration (DLA) (Gahn *et al.*, 1999) constitutes a main contribution to drive electrons with large oscillation in the case of clusterized targets and could reach a value of about 80% of the total energy gain. At the same time modeling of electron acceleration for pure gas media shows that only about 1.5% of the energy gain originates from DLA, whereas the remaining gain was due to laser wake field acceleration.

4. CONCLUSION

In conclusion, high-charge multi-MeV electron bunches generated in LPA experiments using clustered gas targets show suitable characteristics for several applications, among them the development of compact injectors of electrons for conventional accelerators and innovative source for pulsed electron radiography. The results presented indicate that stable and under control MeV electron sources can be setup using a multi-TW laser and supersonic gas-jet.

ACKNOWLEDGEMENTS

The work of A. Faenov and T. Pikuz was partially supported by the RFBR projects 14-22-02089 and 14-02-91171-GFEN_a. The activity of the INO-CNR Pisa group was partially supported from the Italian Ministry of Health through the Project No. GR-2009-1608935 (“Study of Radiobiological and Radiotherapic Effects of a Novel Laser-Driven Electron Accelerator”, D.I. AgeNaS).

REFERENCES

Abdallah, J., Faenov, A.Y., Skobelev, I.Y., Magunov, A.I., Pikuz, T.A., Auguste, T., D’Oliveira, P., Hulin, S. & Monot, P. (2001). Hot-electron influence on the x-ray emission spectra of Ar clusters heated by a high-intensity 60-fs laser pulse. *Phys. Rev. A* **63**, 032706.

Boldarev, A.S., Gasilov, V.A., Faenov, A.Ya., Fukuda, Y. & Yamakawa, V. (2006). Gas-cluster targets for femtosecond laser interaction: Modeling and optimization. *Rev. Sci. Instrum.* **77**, 083112.

Bussolino, G., Faenov, A., Giulietti, A., Giulietti, D., Koester, P., Labate, L., Levato, T., Pikuz, T. & Gizzi, L. (2013). Electron radiography using a table top laser-cluster plasma accelerator, *J. Phys. D: Appl. Phys.* **46**, 245501.

Chair, A.N.R., Blackwell, C.R., Coursey, B.M., Gall, K.P., Galvin, J.M., McLaughlin, W.L., Meigooni, A.S., Nath, R., Rodgers, J.E. & Soares, C.G. (1998). Radiochromic film dosimetry: Recommendations of aapm radiation therapy committee task group 55. *Med. Phys.* **25**, 2093–2115.

Chen, L.M., Yan, W.C., Li, D.Z., Hu, Z.D., Zhang, L., Wang, W.M., Hafz, N., Mao, J.Y., Huang, K., Ma, Y., Zhao, J.R., Ma, J.L., Li, Y.T., Lu, X., Sheng, Z.M., Wei, Z.Y., Gao, J. & Zhang, J. (2013). Bright betatron x-ray radiation from a laser-driven-clustering gas target. *Sci. Rep.* **3**, 1912–1918.

Colgan, J., Abdallah Jr., J., Faenov, A.Ya., Pikuz, T.A., Skobelev, I.Yu., Fortov, V.E., Fukuda, Y., Akahane, Y., Aoyama, M.,

Inoue, N. & Yamakawa, K. (2008). The role of hollow atoms in the spectra of an ultrashort-pulse-laser-driven Ar cluster target. *Laser Par. Beams* **26**, 83–93.

Colgan, J., Abdallah Jr., J., Faenov, A.Ya., Pikuz, T.A., Skobelev, I.Yu., Fukuda, Y., Hayashi, Y., Pirozhkov, A., Kawase, K., Shimomura, T., Kiriyama, H., Kato, Y., Bulanov, S.V. & Kando, M. (2011). Observation and modeling of high resolution spectral features of the inner-shell X-ray emission produced by 10^{-10} contrast femtosecond-pulse laser irradiation of argon clusters. *High Energy Density Phys*. **7**, 77–83.

Faenov, A.Ya., Magunov, A.I., Pikuz, T.A., Skobelev, I.Yu., Giulietti, D., Betti, S., Galimberti, M., Gamucci, A., Giulietti, A., Gizzi, L.A., Labate, L., Levato, T., Tomassini, P., Marques, J.R., Bourgeois, N., Dobosz-Dufrenoy, S., Ceccoti, T., Monot, P., Reau, F., Popoescu, H., D'Oliveira, P., Martin, Ph., Fukuda, Y., Boldarev, A.S., Gasilov, S.V. & Gasilov, V.A. (2008). Non-adiabatic cluster expansion after ultrahsort laser interaction. *Laser Part. Beams* **26**, 69–81

Faenov, A.Y., Pikuz, T.A., Fukuda, Y., Kando, M., Kotaki, H., Homma, T., Kawase, K., Kameshima, T., Pirozkhov, A., Yogo, A., Tampo, M., Mori, M., Sakaki, H., Hayashi, Y., Nakamura Jr., T., Pikuz, S.A., Skobelev, I.Y., Gasilov, S.V., Giulietti, A., Cecchetti, C.A., Boldarev, A.S., Gasilov, V.A., Magunov, A., Kar, S., Borghesi, M., Bolton, P., Daido, H., Tajima, T., Kato, Y. & Bulanov, S.V. (2009). Submicron ionography of nanostructures using a femtosecond-laser-driven-cluster-based source. *Appl. Phys. Lett*. **95**, 101107.

Faenov, A.Ya., Pikuz, T.A., Fukuda, Y., Skobelev, I.Yu., Nakamura, T., Bulanov, S.V., Hayashi, Y., Kotaki, H., Pirozhkov, A.S., Kawachi, T., Chen, L.M., Zhang, L., Yan, W.C., Yuan, D.W., Mao, J.Y., Wang, Z.H., Fortov, V.E., Kato, Y. & Kando, M. (2013). Generation of quantum beams in large clusters irradiated by super-intense, high – contrast femtosecond laser pulses. *Contrib. Plasma Phys*. **53**, 148–160.

Faenov, A.Ya., Skobelev, I.Yu., Pikuz, T.A., Pikuz, S.A., Fortov, V.E., Fukuda, Y., Hayashi, Y., Pirozhkov, A., Kotaki, H., Shimomura, T., Kiriyama, H., Kanazawa, S., Kato, Y., Colgan, J., Abdallah, J. & Kando, M. (2012). X-ray spectroscopy diagnoses of clusters surviving under prepulses of ultraintense femtosecond laser pulse irradiation. *Laser Part. Beams* **30**, 481–488.

Fukuda, Y., Akahane, Y., Aoyama, M., Hayashi, Y., Homma, T., Inoue, N., Kando, M., Kanazawa, S., Kiriyama, H., Kondo, S., Kotaki, H., Masuda, S., Mori, M., Yamazaki, A., Yamakawa, K., Echkina, E.Yu., Inovenkov, I.N., Koga, J. & Bulanov, S.V. (2007). Utrarelativistic electron generation during the intense, ultrashort laser pulse interaction with clusters. *Phys. Lett. A* **363**, 130.

Fukuda, Y., Akahane, Y., Aoyama, M., Inoue, N., Ueda, H., Kishimoto, Y., Yamakawa, K., Faenov, A.Ya., Magunov, A.I., Pikuz, T.A., Skobelev, I.Yu., Abdallah Jr., J., Csanak, G., Boldarev, A.S. & Gasilov, V.A. (2004). Generation of X-rays and energetic ions from micron-sized Ar clusters irradiated by ultrafast, high intensity laser pulses. *Laser Part. Beams* **22**, 215–220.

Fukuda, Y., Faenov, A.Y., Tampo, M., Pikuz, T.A., Nakamura, T., Kando, M., Hayashi, Y., Yogo, A., Sakaki, H., Kameshima, T., Pirozhkov, A.S., Ogura, K., Mori, M., Esirkepov, T., Koga, J., Boldarev, A.S., Gasilov, V.A., Magunov, A.I., Kodama, R., Bolton, P., Kato, Y., Tajima, T., Daido, H. & Bulanov, S. (2009). Energy increase in multi-MeV ion acceleration in the interaction of short pulse laser with a cluster-gas target. *Phys. Rev. Lett*. **103**, 165002.

Gahn, C., Tsakiris, G.D., Pukhov, A., Ter Vehn, J.M., Pretzler, G., Thirolf, P., Habs, D. & Witte, K.J. (1999). Multi-MeVelectron beam generation by direct laser acceleration in high-density plasma channels. *Phys. Rev. Lett*. **83**, 4772–4775.

Gavrilenko, V.P., Faenov, A.Ya., Magunov, A.I., Skobelev, I.Yu., Pikuz, T.A., Kim, K.Y. & Milchberg, H.M. (2006). Observation of modulations in Lyman-alfa profiles of multicharged ions in clusters irradiated by fs laser pulses: Effect of a dynamic electric field. *Phys. Rev. A* **73**, 013203.

Giulietti, D. & Labate, L. (2010). Laser Plasma Acceleration and Related Electromagnetic sources. In *Progress in ultrafast intense laser science* (Yamanouchi, K., Giulietti, A. & Ledingham, K., Eds.), Vol. 5, Chap. 9, pp. 165–185. Heidelberg: Springer.

Hayashi, Y., Pirozhkov, A.S., Kando, M., Fukuda, Y., Faenov, A., Kawase, K., Pikuz, T., Nakamura, T., Kiriyama, H., Okada, H. & Bulanov, S.V. (2011). Efficient generation of Xe K-shell x rays by high-contrast interaction with submicrometer clusters. *Opt. Lett*. **36**, 1614–1616.

Jinno, S., Fukuda, Y., Sakaki, H., Yogo, A., Kanasaki, M., Kondo, K., Faenov, A.Ya., Skobelev, I.Yu., Pikuz, T.A., Boldarev, A.S. & Gasilov, V. (2013). Mie scattering from submicron-sized CO_2 clusters formed in a supersonic expansion of a gas mixture. *Opt. Express* **21**, 20656–20674.

Kim, K.Y., Kumarappan, V., Milchberg, H., Faenov, A.Ya., Magunov, A.I., Pikuz, T.A. & Skobelev, I.Yu. (2006). X-Ray spectroscopy of ~1 cm channels produced by self-focusing pulse propagation in elongated cluster jets. *Phys. Rev. E* **78**, 066463.

Kishimoto, Y., Masaki, T. & Tajima, T. (2002). High energy ions and nuclear fusion in laser–cluster interaction. *Phys. Plasmas* **9**, 589.

Kishimoto, Y. & Tajima, T. (2000). Strong coupling between Clusters and Radiation. In *High-field science* (Tajima, T., Mima, K. & Baldis, H., Eds.), Chap. 3, pp. 83–96. New York: Springer.

Kugland, N.L., Constantin, C.G., Neumayer, P., Chung, H.-K., Collette, A., Dewald, E.L., Froula, D.H., Glenzer, S.H., Kemp, A., Kritcher, A.L., Ross, J.S. & Niemann, C. (2008b). High Kα x-ray conversion efficiency from extended source gas jet targets irradiated by ultra-short laser pulses. *Appl. Phys. Lett*. **92**, 241504.

Kugland, N.L., Neumayer, P., Döppner, T., Chung, H.-K., Constantin, C.G., Girard, F., Glenzer, S.H., Kemp, A. & Niemann, C. (2008a). High contrast Kr gas jet Kα x-ray source for high energy density physics experiments. *Rev. Sci. Instrum*. **79**, 10E917.

Magunov, A.I., Faenov, A.Ya., Skobelev, I.Yu., Pikuz, T.A., Dobosz, S., Schmidt, M., Perdrix, M., Meynadier, P., Gobert, O., Normand, D., Stenz, C., Bagnoud, V., Blasco, F., Roche, J.R., Salin, F. & Sharkov, B.Yu. (2003). X-ray spectra of fast ions from clusters by ultra-short laser pulses. *Laser Part. Beams* **21**, 73–79.

Magunov, A.I., Pikuz, T.A., Skobelev, I.Yu., Faenov, A.Ya., Blasco, F., Dorchies, F., Caillaud, T., Bonte, K., Stenz, C., Salin, F., Loboda, P.A., Litvinenko, I.A., Popova, V.V., Baidin, G.V., Abdallah Jr., J. & Junkel-Vives, G.C. (2001). Influence of ultrashort laser pulse duration on the X-ray emission spectrum of plasma produced in cluster target. *JETP Lett*. **74**, 375–379.

Malka, V., Fritzler, S., Lefebvre, E., Aleonard, M.M., Burgy, F., Chambaret, J.P., Chemin, J.F., Krushelnick, K., Malka, G., Mangles, S.P.D., Najmudin, Z., Pittman, M., Rousseau, J.-P., Scheurer, J.-N., Walton, B. & Dangor, A.E. (2002). Electron

acceleration by a wake field forced by an intense utrashort laser pulse. *Science* **298**, 1596.

Mangles, S., Walton, B., And, Z.N., Dangor, A.E., Krushelnick, K., Malka, V., Manclossi, M., Lopes, N., Carias, C., Mendes, G. & Dorchies, F. (2006). Table-top laser-plasma acceleration as an electron radiography source. *Laser Part. Beams* **24**, 185–190.

Mangles, S.P.D., Genoud, G., Bloom, M.S., Burza, M., Najmudin, Z., Persson, A., Svensson, K., Thomas, A.G.R. & Wahlström, C.G. (2012). Self-injection threshold in self-guided laser wakefield accelerators. *Phys. Rev. ST Accel. Beams* **15**, 011302.

Merrill, F., Harmon, F., Hunt, A., Mariam, F., Morley, K., Morris, C., Saunders, A. & Schwartz, C. (2007). Electron radiography. *Nucl. Instrum. Methods B* **261**, 382–386.

Modena, A., Najmudin, Z., Dangor, A., Clayton, C., Marsh, K., Joshi, C., Malka, V., Darrow, C., Danson, C., Neely, D. & Walsh, F. (1995). Electron acceleration from the breaking of relativistic plasma waves. *Nature* **377**, 606.

Najmudin, Z., Krushelnick, K., Clark, E., Mangles, S., Walton, B., Dangor, A., Fritzler, S., Malka, V., Lefebvre, E., Gordon, D., Tsung, F. & Joshi, C. (2003). Self-modulated wakefield and forced laser wakefield acceleration of electrons. *Phys. Plasmas* **10**, 2071.

Sakabe, S., Shimizu, S., Hashida, M., Sato, F., Tsuyukushi, T., Nishihara, K., Okihara, S., Kagawa, T., Izawa, Y., Imasaki, K. & Iida, T. (2004). Generation of high-energy protons from the Coulomb explosion of hydrogen clusters by intense femtosecond laser pulses. *Phys. Rev. A* **69**, 023203.

Schumaker, W., Nakanii, N., McGuffey, C., Zulick, C., Chyvkov, V., Dollar, F., Habara, H., Kalintchenko, G., Maksimchuk, A., Tanaka, K.A., Thomas, A.G.R., Yanovsky, V. & Krushelnick, K. (2013). Ultrafast electron radiography of magnetic fields in high-intensity laser-solid interactions. *Phys. Rev. Lett.* **110**, 015003.

Serbanescu, C. & Fedosejevs, R. (2006). Electron radiography using hot electron jets from sub-millijoule femtosecond laser pulses. *Appl. Phys. B* **83**, 521–525.

Sherrill, M.E., Abdallah Jr., J., Csanak, G., Dodd, E.S., Fukuda, Y., Akahane, Y., Aoyama, M., Inoue, N., Ueda, H., Yamakawa, K., Faenov, A.Ya., Magnov, A.I., Pikuz, T.A. & Skobelev, I.Yu. (2006). Spectroscopic characterization of an ultrashort laser driven Ar cluster target incorporating both Boltzmann and particle-in-cell models. *Phys. Rev. E* **73**, 066404.

Tajima, T. & Dawson, J. (1979). Laser electron accelerator. *Phys. Rev. Lett.* **43**, 267.

Tajima, T., Kishimoto, Y. & Downer, M.C. (1999). Optical properties of cluster plasma. *Phys. Plasmas* **6**, 3759.

Zhang, L., Chen, L.-M., Yuan, D.-W., Yan, W.-C., Wang, Z.-H., Liu, C.H., Shen, Z.H.-W., Faenov, A., Pikuz, T., Skobelev, I., Gasilov, V., Boldarev, A., Mao, J.-Y., Li, Y.-T., Dong, Q.-L., Lu, X., Ma, J.-L., Wang, W.-M., Sheng, Z.H.-M. & Zhang, J. (2011). Enhanced Kα output of Ar and Kr using size optimized cluster target irradiated by high-contrast laser pulses. *Opt. Express* **19**, 25812–25822.

Zhang, L., Chen, L.M., Wang, W.M., Yan, W.C., Yuan, D.W., Mao, J.Y., Wang, Z.H., Liu, C., Shen, Z.W., Faenov, A., Pikuz, T., Li, D.Z., Li, Y.T., Dong, Q.L., Lu, X., Ma, J.L., Wei, Z.Y., Sheng, Z.M. & Zhang, J. (2012). Electron acceleration via high contrast laser interacting with submicron clusters. *Appl. Phys. Lett.* **100**, 014104.